**2007 年 2 月**

**碩士學位論文**

# Effect of Proline to Peptoid Residue Substitution on the Structure, Cell Selectivity and Mechanism of Antibacterial Action of Antimicrobial Peptide Tritrpticin-amide

朝鮮大學校 大學院

生物新素材學科

朱 萬 龍

# Effect of Proline to Peptoid Residue Substitution on the Structure, Cell Selectivity and Mechanism of Antibacterial Action of Antimicrobial Peptide Tritrpticin-amide

**항균펩타이드 tritrpticin-amide 의 구조, 세포특이성 및 항균작용기작에 있어서 proline 의 peptoid 잔기로의 치환이 미치는 영향**

**2007 年 2 月 日**

朝鮮大學校 大學院

生物新素材學科

朱 萬 龍

# Effect of Proline to Peptoid Residue Substitution on the Structure, Cell Selectivity and Mechanism of Antibacterial Action of Antimicrobial Peptide Tritrpticin-amide

**指導敎授 申 松 曄**

**이 論文을 理學碩士 學位申請 論文으로 提出함.**

**2006 年 10 月 日**

朝鮮大學校 大學院

生物新素材學科

朱 萬 龍

# 朱萬龍의 碩士學位論文을 認准함

委員長 朝鮮大學校 敎授 함 경 수 印

委 員 朝鮮大學校 敎授 박 일 선 印

委 員 朝鮮大學校 敎授 신 송 엽 印

**2006** 年 **11** 月 日

# 朝鮮大學校 大學院

# CONTENTS

# LIST OF TABLES

# LIST OF FIGURES

# ABSTRACT

## Effect of Proline to Peptoid Residue Substitution on the Structure, Cell Selectivity and Mechanism of Antibacterial Action of Antimicrobial Peptide Tritrpticin-amide

By Wan Long Zhu

Advisor: Prof. Song Yub Shin Ph.D.

Department of Bio-Materials,

Graduate School of Chosun University

To investigate the effect of proline → peptoid residue substitution on cell selectivity and the mechanism of antibacterial action of Pro-containing β-turn antimicrobial peptides, tritrpticin-amide (TP, VRRFPWWWPFLRR-$NH_2$) and its peptoid residue-substituted peptides in which two Pro residues at positions 5 and 9 were replaced with Nleu (Leu peptoid residue), Nphe (Phe peptoid residue) or Nlys (Lys peptoid residue) were synthesized, respectively. Peptides with Pro → Nleu (TPl) or Pro → Nphe (TPf) substitution retained antibacterial activity but had significantly higher toxicity to mammalian cells. In contrast, Pro → Nlys (TPk)

substitution increased the antibacterial activity but decreased the toxicity to mammalian cells. Tryptophan fluorescence studies indicated that the cell selectivity of TPk was closely correlated with a preferential interaction with negatively charged phospholipids. Interestingly, TPk was much less effective at causing the leakage of a fluorescent dye entrapped within negatively charged vesicles and depolarizing of the membrane potential of *Staphylococcus aureus* and *Escherichia coli* spheroplasts. Furthermore, confocal laser-scanning microscopy showed that TPk effectively penetrated the membrane of both *E. coli* and *S. aureus* and accumulated in the cytoplasm, whereas TP and TPf did not penetrate the cell membrane but remained outside or on the cell membrane. These results suggest that the bactericidal action of TPk is maybe due to inhibition of the intracellular components after penetration of the bacterial cell membrane. In addition, TPK with Lys substitution induced rapid and effective dye leakage from bacterial membrane-mimicking liposomes. TPK effectively depolarized the membrane potential of *S. aureus* and *E. coli* spheroplasts and did not penetrate the bacterial cell membranes. These results suggested that the ability of TPk to penetrate the bacterial cell membranes appears to involve the dual effects that are related to the increase in the positive charge and the peptide's backbone change by peptoid residue substitution. Collectively, our results showed that Pro → Nlys substitution in Pro-containing β-turn antimicrobial peptides is a promising strategy for the design of new short bacterial cell-selective antimicrobial peptides with intracellular mechanisms of action.

## Ⅰ. INTRODUCTION

Antimicrobial peptides play an important role in the innate immunity system of many higher organisms such as plants, insects, amphibians, and mammals (*1-5*). Due to the alarming emergence of pathogenic organisms resistant to conventional antibiotics, antimicrobial peptides are being intensively studied with the objective of developing a new class of antimicrobial drug. The 13-residue cationic tritrpticin (VRRFPWWWPFLRR) is a member of the cathelicidin family, a group of diverse antimicrobial peptides found in neutrophil granules (*6*). Tritrpticin has a unique composition, consisting of 30% arginine, 23% tryptophan, and 15% proline. Tritrpticin may be a candidate for drug development because it has a broad spectrum of antimicrobial activity against Gram-positive and Gram-negative bacteria and some fungi. Its therapeutic potential, however, is limited by its relatively strong hemolytic activity against human erythrocytes (*6-8*).

Tritrpticin contains two Pro residues at positions 5 and 9. Nuclear magnetic resonance (NMR) study has shown that, in membrane-mimicking sodium dodecyl sulfate (SDS) micelles, tritrpticin adopts a unique structure with two adjacent β-turns around Pro5 and Pro9. The hydrophobic residues are clustered together and are clearly separated from the basic Arg residues, resulting in an amphipathic β-turn structure (*9*). The Pro residue plays a critical role in determining the secondary structure of the peptides because it induces a reversal in backbone conformation, resulting in the breaking of helices as well as in the formation of β-turns. Like Pro, peptoid (*N*-alkylglycyl) residues are imino acids because their side chains are shifted from the α-carbon position to the N-position. Peptoid residue-containing peptides

generally exhibit greater proteolytic stability and bioavailability than their respective peptide analogues (*10*). They have been found to be potential drugs as discovered from peptidomimetic libraries (*11*) and determined to be effective molecular transporters via their enhancement of the cellular uptake of agents (*12*). In another interesting application, the Leu peptoid residue (Nleu) has been introduced as a substituted proline into synthetic collagen-like structures (*13*).

Like proline, peptoid residues have β-turn-forming potential as well as an ability to break α-helices because of they lack an amide proton for forming intramolecular hydrogen bonds (*14*, *15*). To our knowledge, previous studies have not addressed the effect of Pro → peptoid residue substitution on cell selectivity and the mechanism of antibacterial action of amphipathic β-turn antimicrobial peptides containing Pro residues such as tritrpticin. To address these issues, tritrpticin-amide (TP, VRRFPWWWPFLRR-$NH_2$) and its peptoid residue-substituted peptides having the sequence VRRFXWWWXFLRR-$NH_2$ were synthesized, in which X represents substitutions of Pro with Nleu (Leu peptoid residue), Nphe (Phe peptoid residue), or Nlys (Lys peptoid residue).

The cell selectivity of the peptides was assessed by measuring the antimicrobial activity against bacterial strains including antibiotic-resistant clinical isolations and fungal strain, the hemolytic activity against human red blood cells, and the cytotoxicity against human cervical carcinoma HeLa and mouse fibroblastic NIH-3T3 cells. Furthermore, the molecular basis for the cell selectivity of the peptides was investigated by using tryptophan fluorescence spectroscopy and model membrane systems mimicking the bacterial and mammalian cytoplasmic membranes. The secondary structures of the peptides in the SDS micelles were

further examined by circular dichroism (CD) spectroscopy. Additionally, the mechanism of antibacterial action of the peptides was investigated by fluorescent dye leakage, membrane depolarization, confocal laser-scanning microscopy, and gel retardation. These peptoid residue-containing antimicrobial peptides offer unique insight into how peptides interact with model membranes, intact bacterial membranes, or mammalian cell membranes, and the results provide important information about the design of possible cell-selective antimicrobial peptides for therapeutic applications.

## Ⅱ. MATERIALS AND METHODS

### Ⅱ-1. *Materials*

Rink amide 4-methylbenzhydrylamine resin, fluoren-9-yl-methoxycarbonyl (Fmoc)-amino acids, Fmoc-Ahx-OH and other reagents for the peptide synthesis were purchased from Calibochem-Novabiochem (La Jolla, CA). Egg yolk L-α-phosphatidylcholine (EYPC), egg yolk L-α-phosphatidyl-DL-glycerol (EYPG), acrylamide, calcein, 3-(4,5-dimethylthiazol-2-yl)- 2,5-diphenyl-2H-tetrazolium bromide (MTT) and GD (gramicidin D) were supplied by Sigma Chemical Co. (St. Louis, MO). 3, 3'-Dipropylthiadicarbocyanine iodide ($diSC_3$-5) was obtained from Molecular Probes (Eugene, OR). DMEM and fetal bovine serum (FBS) were supplied from HyClone (SeouLin Bioscience, Korea). Human cervical carcinoma HeLa and mouse fibroblastic NIH-3T3 cells were purchased from the American Type Culture Collection (Manassas, VA). All other reagents were analytical grade. The buffers were prepared in double glass-distilled water.

### Ⅱ-2. *Peptide Synthesis and purification*

Tritrpticin-amide and its peptoid-containing peptides and FITC-labeled peptides (FITC-labeled aminocaproic acid-peptides) were prepared by the standard Fmoc-based solid-phase method on rink amide 4-methylbenzhydrylamine resin (0.54 mmole/g). Fmoc-Nleu-OH, Fmoc-Nphe-OH, and Fmoc-Nlys-OH were synthesized using the previous methods (*14, 15*).

The crude peptides were purified by RP-HPLC using a Shim-pack $C_{18}$ column (15 μm, 20 mm × 250 mm Shimadzu, Japan). The purified peptides were shown to be homogeneous (> 98%) by analytical RP-HPLC on a Shim-pack $C_{18}$ column (5 μm, 4.6 mm × 250 mm Shimadzu, Japan). Matrix-assisted laser-desorption ionization-time-of-flight mass spectrometry (MALDI-TOF MS) (Shimadzu, Japan) was used to confirm their molecular weight (Table 1).

### Ⅱ-3. *Microorganisms*

Three Gram-positive bacterial strains [*Bacillus subtilis* (KCTC 3068), *Staphylococcus epidermidis* (KCTC 1917) and *Staphylococcus aureus* (KCTC 1621)], three Gram-negative bacterial strains [*Escherichia coli* (KCTC 1682), *Salmonella typhimurium* (KCTC 1926) and *Pseudomonas aeruginosa* (KCTC 1637)] and one fungal strain [*Candida albicans* (KCTC 7965)] were purchased from the Korean Collection for Type Cultures (KCTC) at Korea Research Institute of Bioscience & Biotechnology (KRIBB) in Korea. Two antibiotic-resistant *Staphylococcus aureus* (CCARM 3089 and CCARM 3108) and two antibiotic-resistant *Escherichia coli* (CCARM 1129 and CCARM 1238) were obtained from the Culture Collection of Antibiotic-Resistant Microbes (CCARM) at Seoul Women's University in Korea.

### Ⅱ-4. *Antimicrobial activity assay*

In antimicrobial activity assay, the broth microdilution method was used. Briefly, single colonies of bacteria or fungi were inoculated into the culture medium (LB broth for bacteria

and YM broth for *C. albicans*) and cultured overnight at 37 °C (or 30 °C for *C. albicans*). An aliquot of this culture was transferred to fresh culture medium and incubated for an additional 3-5 h at 37 °C (for bacteria) or 30 °C (for *C. albicans*) to obtain mid-logarithmic phase organisms. Aliquots (100 μL) of a bacterial suspension at $2 \times 10^6$ colony-forming units (CFU)/mL in 1% peptone were added to 100 μL of a peptide solution (serial 2-fold dilutions in 1% peptone). After incubation for 18–20 h at 37 °C (or 30 °C for *C. albicans*), the inhibition of bacterial growth was assessed by measuring absorbance at 620 nm with a Microplate ELISA Reader EL 800 (Bio-Tek Instruments). The minimal inhibitory concentration (MIC) was defined as the lowest concentration of peptide that inhibited the microorganism growth.

### Ⅱ-5. *Hemolytic activity assay*

Hemolytic activity of the peptides against human red blood cells (h-RBCs) was tested. Fresh h-RBCs were washed three times with phosphate-buffered saline (PBS) [35 mM phosphate buffer containing 150 mM NaCl, pH 7.4] by centrifugation for 10 min at 1000g and resuspended in PBS. The peptide solutions (serial 2-fold dilutions in PBS) were then added to 50 μL of h-RBC in PBS to give a final volume of 100 μL and a final erythrocyte concentration of 4% (v/v). The resulting suspension was incubated with agitation for 1h at 37 °C. The samples were centrifuged at 1000g for 5 min. Release of hemoglobin was monitored by measuring the absorbance of the supernatant at 405 nm. Controls for no

hemolysis (blank) and 100% hemolysis consisted of human red blood cells suspended in PBS and 0.1% Triton-X 100, respectively.

### Ⅱ-6. *Cytotoxicity against mammalian cells*

Human cervical carcinoma HeLa and mouse fibroblastic NIH-3T3 cells were cultured in DMEM with 10% FBS. The cells were maintained under 5% $CO_2$ at 37 ℃. Cytotoxicity against mammalian cells of the peptides was determined by the MTT assay as previously reported (*16*) with minor modifications. The cells were seeded on 96-well microplates at a density of $2 \times 10^4$ cells/well in 150 μL of DMEM containing 10% FBS. The plates were then incubated for 24 h at 37 ℃ in a 5% $CO_2$ atmosphere. 20 μL of peptide solution (serial 2-fold dilutions in DMEM) were added, and the plates were incubated for a further 2 days. Wells containing cells without peptides served as controls. Subsequently, 20 μL of an MTT solution (5 mg/mL) was added to each well, and the plates were incubated for a further 4 h at 37 ℃. The precipitated MTT formazan was dissolved in 40 μL of 20% (w/v) SDS containing 0.01 M HCl overnight. The absorbance at 570 nm was measured using a microplate ELISA reader (Molecular Devices, Sunnyvale, CA). Percent cell survival was expressed as a percent ratio of $A_{570}$ of cells treated with peptide over cells only.

### Ⅱ-7. *Circular dichroism (CD) spectroscopy*

The CD spectra of peptides were recorded in sodium phosphate buffer in the presence of 30 mM SDS by utilizing a Jasco J-715 CD spectrophotometer (Tokyo, Japan). The samples were scanned at room temperature in a capped quartz cuvette of 1-mm path length cells in the wavelength range of 250-190 nm.

### Ⅱ-8. *Preparation of small unilamellar vesicles (SUVs)*

Small unilamellar vesicles were prepared by a standard procedure with required amounts of either EYPC/EYPG (7:3, w/w) or EYPC/cholesterol (10:1, w/w) for tryptophan fluorescence. Dry lipids were dissolved in chloroform in a small glass vessel. Solvents were removed by rotary evaporation to form a thin film on the wall of a glass vessel. The dried thin film was resuspended in Tris-HCl buffer by vortex mixing. The lipid dispersions were then sonicated in an ice/water mixture for 10-20 min with a titanium-tip ultrasonicator until the solution became transparent.

### Ⅱ-9. *Tryptophan fluorescence blue shift*

In the tryptophan fluorescence, small unilamellar vesicles (SUVs) were used to minimize differential light scattering effects (*17*, *18*). The tryptophan fluorescence measurements were taken with a model RF-5301PC spectropho tometer (Shimadzu, Japan). Each peptide (final concentration of 3 μM) was added to 3 ml of Tris buffer [10mM Tris, 0.1 mM EDTA, 150 mM NaCl, pH 7.4] containing 0.6 mM liposomes, and the peptide/liposome mixture was

allowed to interact at 20 °C for 10 min. Tryptophan residues of each peptide were excited at 280 nm, and the emission spectra were recorded from 300 to 400 nm.

### Ⅱ-10. *Tryptophan fluorescence quenching by acrylamide*

Acrylamide quenching experiments were carried out at an excitation wavelength of 295 nm instead of 280 nm to reduce absorbance by acrylamide and emission spectrum was 330 nm (*19, 20*). Aliquots of the 4.0 M solution of this water-soluble quencher were added to the peptide in the absence or presence of liposomes at a peptide:lipid molar ratio of 1:200. The acrylamide concentration in the cuvette was from 0.04 to 0.21 M. The effect of acrylamide on the fluorescence of each peptide was analyzed with a Stern-Volmer equation:

$$F_0/F = 1 + K_{sv}[Q]$$

where $F_0$ and $F$ represent the fluorescence insensitivities of the peptide in the absence and the presence of acrylamide, respectively, $K_{sv}$ is the Stern-Volmer quenching constant, and [Q] is the concentration of acrylamide.

### Ⅱ-11. *Preparation of calcein-loaded LUVs and leakage assay*

Calcein-entrapped LUVs composed of EYPC/EYPG (7:3, w/w) were prepared by vortexing the dried lipid in dye buffer solution [70 mM calcein, 10mM Tris, 150 mM NaCl,

and 0.1 mM EDTA (pH 7.4)]. The suspension was frozen and thawed in liquid nitrogen for ten cycles and extruded through polycarbonate filters (two stacked 100 nm pore size filters) with a LiposoFast extruder (Avestin, Inc. Canada). Untrapped calcein was removed by gel filtration on a Sephadex G-50 column. Usually lipid vesicles are diluted to approximately 10-fold after passing through a Sephadex G-50 column. The eluted calcein-entrapped vesicles were diluted further to the desired final lipid concentration for the experiment. The leakage of calcein from the LUVs was monitored by measuring the fluorescence intensity at an excitation wavelength of 490 nm and an emission wavelength of 520 nm on a model RF-5301PC spectrophotometer (Shimadzu, Japan). For determination of 100% dye-release, 10% Triton-X 100 in Tris-buffer (20 μL) was added to dissolve the vesicles. The percentage of dye-leakage caused by the peptides was calculated as follows:

$$\% \text{ Dye leakage} = 100 \times [(F - F_0) / (F_t - F_0)]$$

where $F$ is the fluorescence intensity achieved by the peptides and $F_0$ and $F_t$ are fluorescence intensities without the peptides and with Triton X-100, respectively.

### Ⅱ-12. *Membrane depolarization assay with bacteria*

The membrane depolarization activity of the peptides was determined with Gram-positive bacteria and Gram-negative bacterial spheroplasts using the experimental conditions described previously (*21, 22*). Gram-positive bacteria, *S. aureus*, was grown at 37 °C with

agitation to mid-log phase ($OD_{600}$ = 0.4). The cells were centrifuged, washed twice with buffer [20 mM glucose and 5 mM HEPES (pH 7.4)], and resuspended to an $OD_{600}$ of 0.05 in a similar buffer containing 0.1 M KCl. Spheroplasts of Gram-negative *E. coli* bacteria (lipopolysaccharide- and peptidoglycan-free bacteria) were prepared by the osmotic shock procedure as follows. Cells from cultures grown to an $OD_{600}$ of 0.8 were harvested by centrifugation and washed twice with buffer [10 mM Tris-$H_2SO_4$ and 25% sucrose (pH 7.5)], and resuspended in the similar buffer containing 1 mM EDTA. After a 10 min incubation at 20 °C with rotary mixing, the cells were collected by centrifugation and resuspended immediately in cold (4 °C) water. After a 10 min incubation at 4 °C with rotary mixing, the spheroplasts were then collected by centrifugation. The spheroplasts were then resuspended to an $OD_{600}$ of 0.1 in a buffer containing 20 mM glucose, 5 mM HEPES, and 0.1 M KCl (pH 7.4). The prepared cells of *S. aureus* or *E. coli* spheroplasts were incubated with 20 nM di$SC_3$-5 until a stable reduction of fluorescence was achieved (around 60 min), indicating the incorporation of the dye into the bacterial membrane. The peptides were then added from the stock solution (1 mg/mL) and dissolved in the buffer to achieve the desired concentration. Membrane depolarization was monitored by the change in the intensity of fluorescence emission of the membrane potential-sensitive dye di$SC_3$-5 (excitation wavelength $\lambda_{ex}$ = 622 nm; emission wavelength $\lambda_{em}$ = 670 nm) after different concentrations of peptides were added. Full dissipation of the membrane potential was obtained by adding gramicidin D (for *S. aureus*, the final concentration is 0.2 nM) or melittin (for *E. coli* spheroplasts, the final concentration is 0.5 μM). The membrane potential dissipating activity of the peptides is expressed as follows:

$$\% \text{ inhibition} = 100 \times [(F_p - F_0) / (F_g - F_0)]$$

where $F_0$ is the stable fluorescence value after addition of the $diSC_3$-5 dye, *Fp* is the fluorescence value 2 min after addition of the peptides, and *Fg* the fluorescence value after the addition of gramicidin D (for *S. aureus*) or melittin (for *E. coli* spheroplasts).

.

### Ⅱ-13. *Confocal laser-scanning microscope in bacterial strains*

*E. coli* and *S. aureus* cells in mid-logarithmic phase were prepared. *E. coli* and *S. aureus* cells ($10^7$ CFU/mL) in 10 mM sodium phosphate buffer (NAPB, pH 7.4) were incubated with FITC-labeled peptides (5 μg/mL) at 37 ℃ for 30 min. After being incubated, the cells were washed with 10 mM NAPB and immobilized on a glass slide. The FITC-labeled peptides were observed with an Olympus IX 70 confocal laser-scanning microscope (Japan). Fluorescent images were obtained with a 488 nm band-pass filter for excitation of FITC.

### Ⅱ-14. *DNA binding assay*

Gel retardation experiments were performed by mixing 100 ng of the plasmid DNA (pBluescript II $SK^+$) with increasing amounts of peptide in 20 μL of binding buffer [5% glycerol, 10 mM Tris-HCl (pH 8.0), 1 mM EDTA, 1 mM dithiothreitol, 20 mM KCl, and 50 g/ml bovine serum albumin]. The reaction mixtures were incubated at room temperature for

1 h. Subsequently, 4 μL of native loading buffer was added [10% Ficoll 400, 10 mM Tris-HCl (pH 7.5), 50 mM EDTA, 0.25% bromophenol blue, and 0.25% xylene cyanol] and a 20 μL aliquot was subjected to a 1% agarose gel electrophoresis in 0.5 × Tris borate-EDTA buffer [45 mM Tris-borate and 1 mM EDTA (pH 8.0)]. The plasmid DNA used in this experiment was purified by CsCl-gradient ultracentrifugation to select the closed circular form of the plasmid.

### Ⅱ-15. *Peptide internalization and visualization in mammalian cells by confocal laser-scanning microscope*

HeLa cells ($10^5$ cells/mL) were seeded on a 12-well culture plate (1 mL/well) and cultured for 16 h. After complete adhesion, the culture medium was discarded, and the cells were washed once with PBS. The cells were pre-incubated in 1 mL fresh DMEM medium (FBS-free) at 37 ℃ for 30 min before incubation with the peptides. Then, the cells were incubated at 37 ℃ with 1 mL fresh DMEM medium (FBS-free) containing FITC-labeled peptides. The final concentration of the peptides was 4 μM. After 30 min, cells were washed three times with PBS and then were mounted with an Olympus IX 70 confocal laser-scanning microscope (Japan). Fluorescent images were obtained with a 488 nm band-pass filter for excitation of FITC.

## Ⅲ. RESULTS

### Ⅲ-1. *Peptide design*

To investigate the effect of Pro → peptoid residue substitution in tritrpticin-amide on cell selectivity and the mechanism of antibacterial action, tritrpticin-amide (TP, VRRFPWWWPFLRR-$NH_2$) and its peptoid residue-substituted peptides having the sequence VRRFXWWWXFLRR-$NH_2$ were synthesized, in which X represents substitutions of Pro with Nleu (Leu peptoid residue), Nphe (Phe peptoid residue), or Nlys (Lys peptoid residue). In addition, to compare the effect of Pro → Nlys substitution and Pro → Lys substitution in tritrpticin-amide on their biological activity and mode of antibacterial action, TPK in which two Pro residues were replaced with two lysine residues was synthesized. The amino acid sequences of all peptides are summarized in Table 1.

### Ⅲ-2. *Antimicrobial activities*

The antimicrobial activities of the peptides against six bacterial strains including three Gram-negative and three Gram-positive species, one fungal strain and four antibiotic-resistant *S. aureus* and *E. coli* strains were investigated using the broth microdilution method (*23-25*). The MIC values of the peptides against these microbial strains are summarized in Table 2. TPl and TPf exhibited antimicrobial activities similar to those of TP against all of the bacterial strains that were tested. In contrast, TPk and TPK exhibited 2-4-fold higher activity than TP.

In addition, the antimicrobial activities of peptides against antibiotic-resistant clinical isolates were also investigated. All of the peptides have effective antimicrobial activities against these antibiotic-resistant clinical isolates at the range of 1-8 μM (Table 3). Noticeably, TPk had the highest antimicrobial activity compared to other peptides.

### Ⅲ-3. *Hemolytic activities*

The hemolytic activity of the peptides against human erythrocytes was also determined. The dose-response curves for the hemolytic activities of the peptides are shown in Figure 1. TPl and TPf exhibited greater hemolytic activity than TP, whereas TPk and TPK exhibited decreased hemolytic activity. Interestingly, TPk did not cause any hemolysis at 200 μM, but TPK caused 20% hemolysis.

### Ⅲ-4. *Cytotoxicity against mammalian cells*

The abilities of the peptides to inhibit the growth of two mammalian cell lines (human cervical carcinoma HeLa and mouse fibroblastic NIH-3T3 cells) were examined to investigate the cytotoxicity of peptides against mammalian cells. The growth inhibition dose-response curves for the peptides were shown in Figure 2. The $IC_{50}$ is the peptide concentration causing 50% inhibition of cell growth compared to untreated control cells (Table 4). TPl, TPf, and TPK were much more cytotoxic than TP and TPk. In particular, TPk was not cytotoxic against HeLa and NIH-3T3 cell lines even at 100 μM (Figure 2).

### Ⅲ-5. *CD spectroscopy*

The secondary structures of the peptides in the presence of 30 mM SDS was next determined by CD spectroscopy (Figure 3). The CD spectra of TP, TPl, and TPf showed a positive band at near 212 nm, suggesting a characteristic β-turn conformation, and a negative band at near 225 nm, which was due to the interaction of the tryptophan side chain with the backbone of its nearest-neighbor residues (*26*). In contrast, the CD spectrum of TPK showed two negative minimum bands at near 208 nm and 222 nm and a positive maximum band at 195 nm, suggesting an α-helical structure. Interestingly, the CD spectrum of TPk displayed no signal at 212 nm, suggesting the disappearance of β-turn structure, but a negative band at near 203 nm and a positive band at near 220 nm, suggesting a poly-L-proline II helix conformation (*27*).

### Ⅲ-6. *Tryptophan fluorescence blue shift*

The fluorescence emission of each peptide's tryptophan residue in Tris-buffer or in the presence of vesicles composed of either negatively charged phospholipids [EYPC/EYPG (7:3, w/w) SUVs], which mimic bacterial membranes, or zwitterionic phospholipids [EYPC/cholesterol (10:1, w/w) SUVs], which mimic mammalian membranes were monitored to determine the local environments of the peptides (Table 5). In the negatively charged vesicles, all of the peptides exhibited similar large blue shifts in their emission maxima,

suggesting that the Trp residue in all of the peptides inserts into the more hydrophobic environment of the membrane interior. In the zwitterionic phospholipid vesicles, TP, TPl, TPf, and TPK exhibited much larger blue shifts in their emission maxima than TPk, suggesting that the Trp residue of TPk more shallowly inserts itself into the membrane interior than TP, TPl, TPf, and TPK.

### Ⅲ-7. *Tryptophan fluorescence quenching studies*

The fluorescence quenching experiment using the water-soluble neutral fluorescence quencher acrylamide in SUVs was performed to investigate the relative extent of peptide burial in the model membranes. The Stern-Volmer plots for the quenching of tryptophan recorded by acrylamide in the absence and presence of lipid vesicles are shown in Figure 4. The fluorescence of typtophan of the peptides decreased in a concentration-dependent manner via the addition of acrylamide to the peptide solution both in the absence and in the presence of liposomes. However, compared with the measurements in the absence of liposomes, the slopes were decreased in the presence of EYPC/EYPG (7:3, w/w) SUVs or EYPC/cholesterol (10:1, w/w) SUVs, suggesting that tryptophan of the peptides was buried in the bilayers, becoming inaccessible for quenching by acrylamide. In the presence of EYPC/EYPG (7:3, w/w) SUVs, all of the peptides exhibited similar extents of quenching, suggesting that their Trp residues are buried effectively in the negatively charged phospholipid membranes. In contrast, the order for the relative extent of quenching of the tryptophan fluorescence in the presence of EYPC/cholesterol (10:1, w/w) SUVs was as follows: TPk > TPK > TP >> TPl >

TPf, suggesting the Trp residue of TPk is less able to insert into the hydrophobic core of zwitterionic phospholipid membranes than that of TPf (Table 5). In particular, the slope for TPk in the presence of EYPC/cholesterol (10:1, w/w) SUVs was much higher than in the presence of EYPC/EYPG (7:3, w/w) SUVs, suggesting TPk has a preferential interaction with negatively charged phospholipids.

### Ⅲ-8. *Peptide-induced dye leakage from negatively charged LUVs*

The ability of the peptides to release the fluorescent marker calcein from calcein-entrapped bacterial cell membrane-mimicking negatively charged EYPC/EYPG (7:3, w/w) LUVs was assessed to determine the membrane disruption activity of the peptides. The does-dependent and time-dependent response curves of peptide-induced calcein leakage from negatively charged vesicles are shown in panels A and B of Figure 5, respectively. TPk induced little or no calcein release, whereas TP, TPl, TPf and TPK exhibited relatively strong membrane-lytic activity. Even at a high concentration of 10 μM, TPk did not cause any dye-leakage. These results further confirm that, whereas membrane disruption represents a major killing event for TP, TPl, TPf and TPK, TPk apparently exerts its bactericidal effect in some other way.

### Ⅲ-9. *Membrane potential depolarization*

The ability of the peptides to cause membrane depolarization of *S. aureus* and *E. coli* spheroplasts using the membrane potential-sensitive dye diSC3-5 was evaluated to determine

the extent to which permeabilization of the cytoplasmic membrane contributed to the antibacterial activity of the peptides (Figure 6). Upon addition of the dye to a suspension of *S. aureus* and *E. coli* spheroplasts, its fluorescence was strongly quenched as it entered the membrane until levels within the membrane stabilized. Subsequent addition of peptides resulted in an increase in di$SC_3$-5 fluorescence reflecting the membrane depolarization, after which addition of gramicidin D (for *S. aureus*) or melittin (for *E. coli* spheroplasts) fully collapsed the membrane potential. TP, TPl, TPf, and TPK depolarized *S. aureus* and *E. coli* spheroplasts at a concentration of 2-4 μM, strongly suggesting that the bacterial cytoplasmic membrane is a major target of these peptides. In contrast, TPk caused very little depolarization at a concentration of 2-4 μM (2-fold MIC), suggesting that the antibacterial activity of TPk is not due to permeabilization of the bacterial cell membrane.

### Ⅲ-10. *Confocal laser-scanning microscopy in bacterial strains*

To determine the site of action of the peptides, Gram-negative E. coli and Gram-positive S. aureus were incubated with FITC-labeled peptides and then their localization in bacterial strains were visualized by confocal laser-scanning microscopy (Figures 7 and 8). FITC-labeled TPk penetrated the membranes and accumulated in the cytoplasm of both Gram-negative *E. coli* and Gram-positive *S. aureus.* This finding indicates that the cytoplasm and not the membrane is the major site of action of TPk. In contrast, under the same conditions, FITC-labeled TP, TPf and TPK did not penetrate but remained associated with the membranes.

### Ⅲ-11. *DNA binding activity*

The DNA binding properties of the peptides were examined to attempt to determine their molecular mechanisms of action. The DNA binding affinities of the peptides were determined by analyzing the electrophoretic mobility of DNA bands at various peptides: DNA weight ratios. TPk and TPK similarly inhibited the migration of DNA at concentrations at 2-4 μM. In contrast, TP, TPl, and TPf inhibited the migration of DNA at 8-16 μM (Figure 9).

### Ⅲ-12. *Confocal laser-scanning microscopy in HeLa cells*

Because the mammalian cell penetration properties and antimicrobial activity can coexist in cell-penetrating peptides (CPPs) and our TPk can penetrate into the bacterial strains, it has interest to research TPk's penetrating efficiency in mammalian cells. The location of FITC-labled TP, TPf and TPk in Hela cells were visualized by confocal laser-scanning microscopy, respectively (Figure 10). Results showed that TPk exactly had penetrating efficiency in Hela cells at 37 °C. However, TP and TPf cann't penetrate cell membrane into cytoplasm at 37 °C. In the case of TPk, its internalization mechanism and exact intracellular location still plausible, so the additional experiments must be performed to solve all of these problems.

## Table 1

Amino acid sequences of Tritrpticin-amide and its peptoid residue-substituted peptides[a]

| Peptide | Sequence | Molecular mass (Da) | |
|---|---|---|---|
| | | Calculated | Observed[b] |
| Tritrpticin | VRRFPWWWPFLRR | 1902.2 | 1903.3 |
| TP | VRRFPWWWPFLRR-$NH_2$ | 1901.2 | 1903.2 |
| TPl | VRRF**l**WWW**l**FLRR-$NH_2$ | 1933.3 | 1935.3 |
| TPf | VRRF**f**WWW**f**FLRR-$NH_2$ | 2001.4 | 2002.0 |
| TPk | VRRF**k**WWW**k**FLRR-$NH_2$ | 1963.3 | 1965.2 |
| TPK | VRRFKWWWKFLRR-$NH_2$ | 1963.3 | 1963.4 |

[a]**l**: Nleu [$(CH_3)_2$-CH-NH-$CH_2$-COOH)], **f**: Nphe ($H_5C_6$-$CH_2$-NH-$CH_2$-COOH), **k**: Nlys [$NH_2$-$(CH_2)_4$-NH-$CH_2$-COOH].

[b]Molecular masses of the peptides observed from MALDI-TOF MS.

## Table 2

Minimal inhibitory concentration of the peptides against bacterial strains

| Microorganisms | Minimal Inhibitory Concentration (μM) | | | | | |
|---|---|---|---|---|---|---|
| | Tritrpticin | TP | TPl | TPf | TPk | TPK |
| ***Gram-negative bacteria*** | | | | | | |
| *E. coli* | 8 | 8 | 8 | 8 | 2 | 2 |
| *P. aeruginosa* | 16 | 8 | 16 | 8 | 4 | 4 |
| *S. typhimurium* | 16 | 8 | 16 | 8 | 4 | 2 |
| ***Gram-positive bacteria*** | | | | | | |
| *B. subtilis* | 4 | 1 | 1 | 1 | 1 | 0.5 |
| *S. epidermidis* | 4 | 1 | 1 | 1 | 1 | 0.5 |
| *S. aureus* | 4 | 2 | 2 | 2 | 1 | 1 |
| ***Fungus*** | | | | | | |
| *C. albicans* | 32 | 16 | 16 | 32 | 4 | 2 |

[a] Each MIC was determined in three independent experiments performed in triplicate with a standard deviation of 9.8 %.

## Table 3

Minimal inhibitory concentration of the peptides against antibiotic-resistant bacterial strains[a]

| Peptide | Minimal Inhibitory Concentration (μM)[b] | | | |
|---|---|---|---|---|
| | *E. coli* | | *S. aureus* | |
| | CCARM 1229 | CCARM 1238 | CCARM 3089 | CCARM 3108 |
| TP | 4 | 4 | 1 | 1 |
| TPl | 2 | 2 | 1 | 1 |
| TPf | 4 | 4 | 1 | 1 |
| TPk | 1 | 1 | 1 | 1 |
| TPK | 1 | 2 | 1 | 1 |

[a]Bacterial strains were clinically isolated at the Culture Collection of Antibiotic-resistant Microbes. Oxacillin was inactive at 256 μM for *E. coli* CCARM 1229 and CCARM 1238, and *S. aureus* CCARM 3089 and CCARM 3108.

[b]Each MIC was determined in two independent experiments performed in triplicate with a standard deviation of 7.0 %

**Table 4**

Cytotoxicities of the peptides against mammalian cells[a]

| Peptide | $IC_{50}$ ($\mu$M) | |
|---|---|---|
| | HeLa | NIH-3T3 |
| TP | 70 | >100 |
| TPl | 18 | 52 |
| TPf | 8 | 48 |
| TPk | >100 | >100 |
| TPK | 24 | 32 |

[a]The $IC_{50}$ values were defined as the concentration of peptides to cause 50% cell growth inhibition by the MTT assay.

## Table 5

Tryptophan fluorescence emission maxima of the peptides in Tris-HCl buffer (pH 7.4) or in the presence of EYPC/EYPG (7:3, w/w) and EYPC/Cholesterol (10:1, w/w) liposomes

| Peptide | Tris-HCl buffer (nm) | EYPC/EYPG (7:3, w/w) (nm)[a] | EYPC/cholesterol (10:1, w/w) (nm)[a] | $K_{SV}$ ($M^{-1}$)[b] | |
|---|---|---|---|---|---|
| | | | | EYPE/EYPG (7:3) | EYPC/cholesterol (10:1) |
| TP | 346.6 | 335.6 (11.0) | 338.2 (8.4) | 2.64 | 3.52 |
| TPl | 390.0 | 338.8 (10.8) | 339.2 (9.8) | 2.88 | 2.58 |
| TPf | 350.0 | 340.0 (10.0) | 341.2 (8.8) | 2.71 | 2.18 |
| TPk | 349.6 | 342.4 (7.2) | 346.0 (3.6) | 2.79 | 3.92 |
| TPK | 349.6 | 339.4 (10.2) | 342.6 (7.0) | 2.56 | 3.62 |

[a]: Blue shifts in emission maxima in parentheses.

[b]: Ksv is the Stern-Volmer quenching constant.

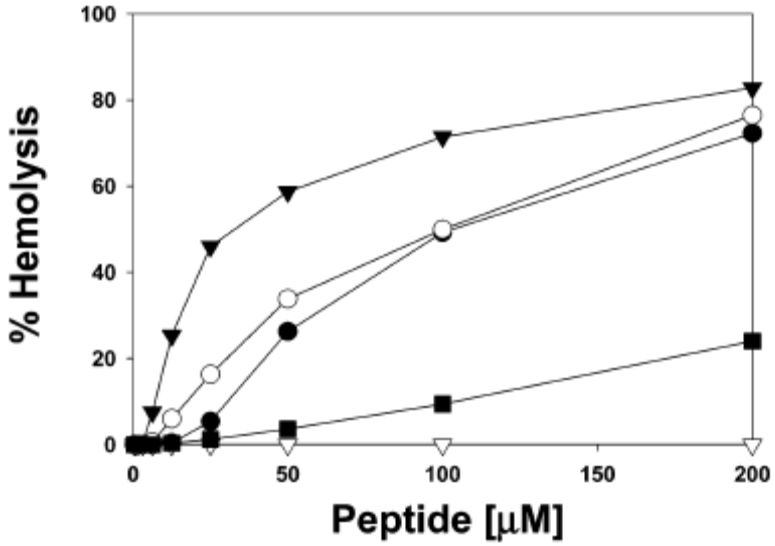


**Figure 1.** Dose-response curves of the hemolytic activity of the peptides toward human erythrocytes: TP (●), TPl (○), TPf (▼), TPk(▽), and TPK (■).

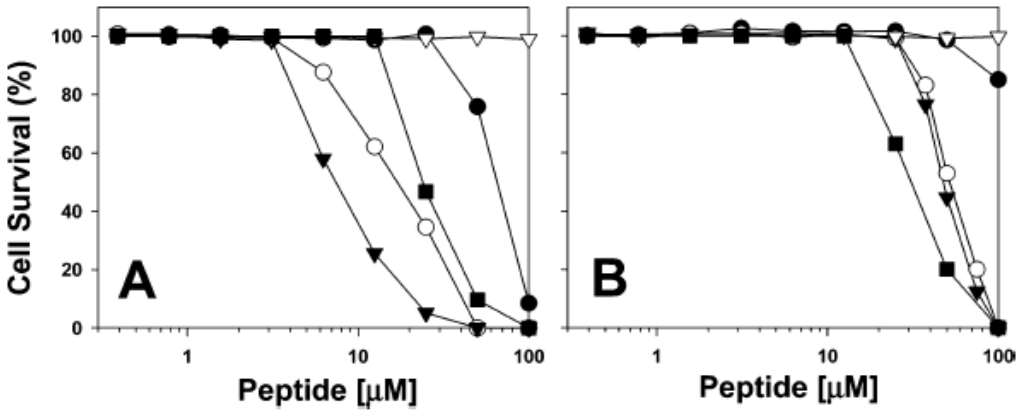


**Figure 2.** Growth inhibition dose-response curves for the peptides against HeLa cells (A) and NIH-3T3 cells (B): TP (●), TPl (○), TPf (▼), TPk(▽), and TPK (■).

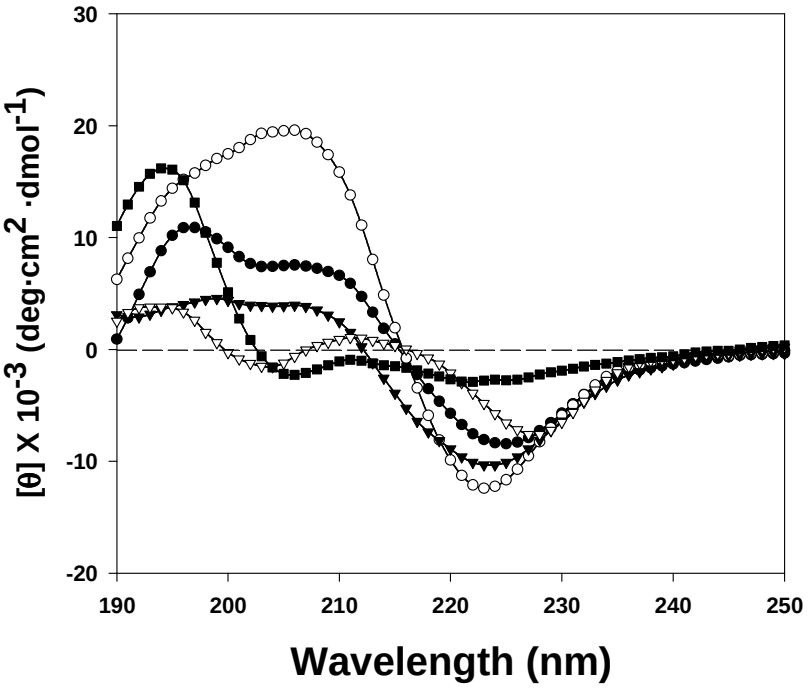


**Figure 3.** CD spectra of the peptides in 10 mM sodium phosphate buffer (pH 7.2) in the presence of 30 mM SDS: TP (●), TPl (○), TPf (▼), TPk (▽), and TPK (■).

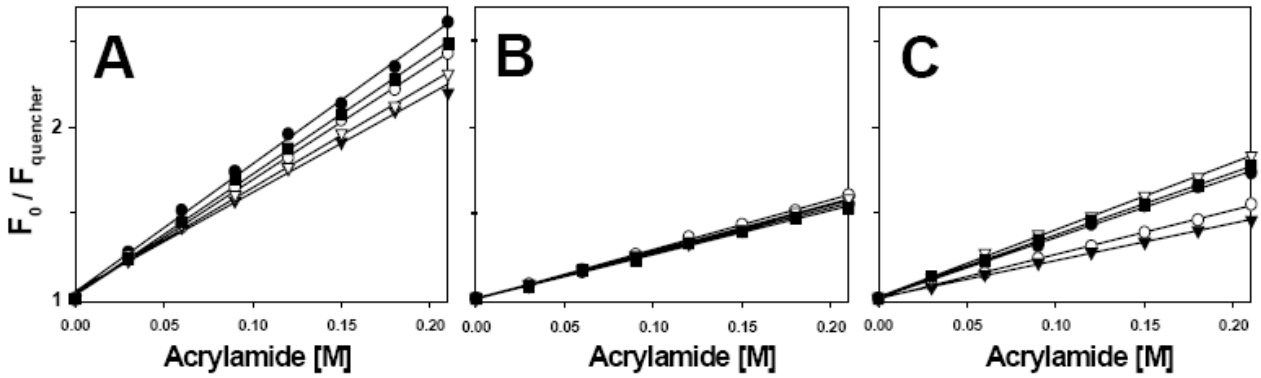


**Figure 4.** Stern-Volmer plots for the quenching of Trp fluorescence of the peptides by an aqueous quencher, acrylamide, in Tris-HCl buffer (pH 7.4) (A) or in the presence of EYPC/EYPG (7:3, w/w) SUVs (B) or EYPC/cholesterol (10:1, w/w) SUVs (C) : TP (●), TPl (○), TPf (▼), TPk(▽), and TPK (■).

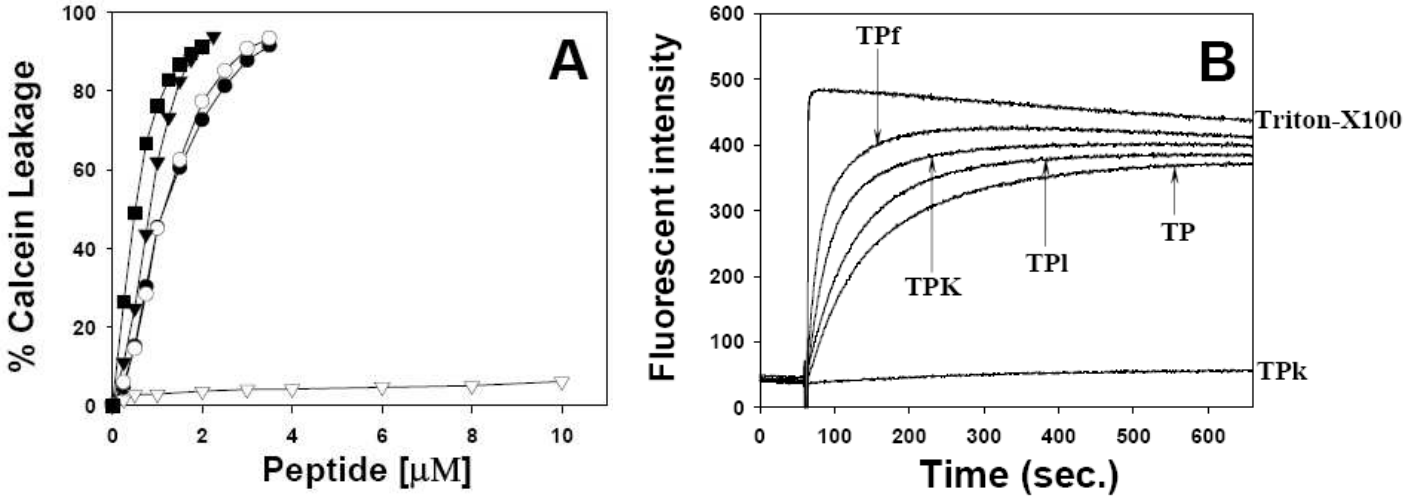


**Figure 5.** (A) The dose-dependent percent leakage of calcein from negatively charged EYPC/EYPG (7:3, w/w) LUVs at pH 7.4 measured at 2 min after the addition the peptides: TP (●), TPl (○), TPf (▼), TPk(▽), and TPK (■). (B) The time-dependent percent leakage of calcein from negatively charged EYPC/EYPG (7:3, w/w) LUVs at pH 7.4 in the presence of 2 μM peptides.

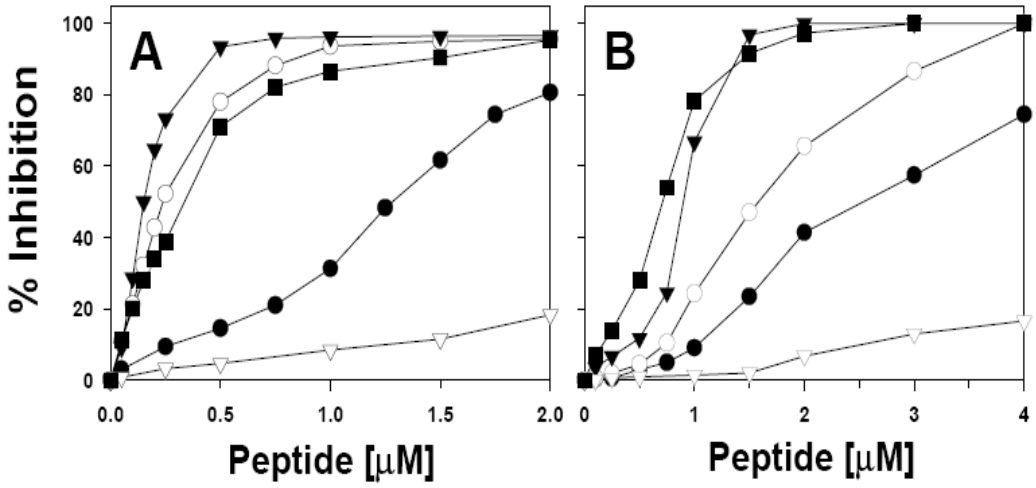


**Figure 6.** Dose-response curves of the membrane depolarization activities of the peptides against *S. aureus* (A) and *E. coli* spheroplasts (B). Membrane depolarization was monitored by an increase in the fluorescence of $diSC_3$-5 (excitation wavelength $\lambda_{ex}$=622nm; emission wavelength $\lambda_{em}$=670nm) after the addition of peptides at different concentrations: TP (●), TPl (○), TPf (▼), TPk(▽), and TPK (■).

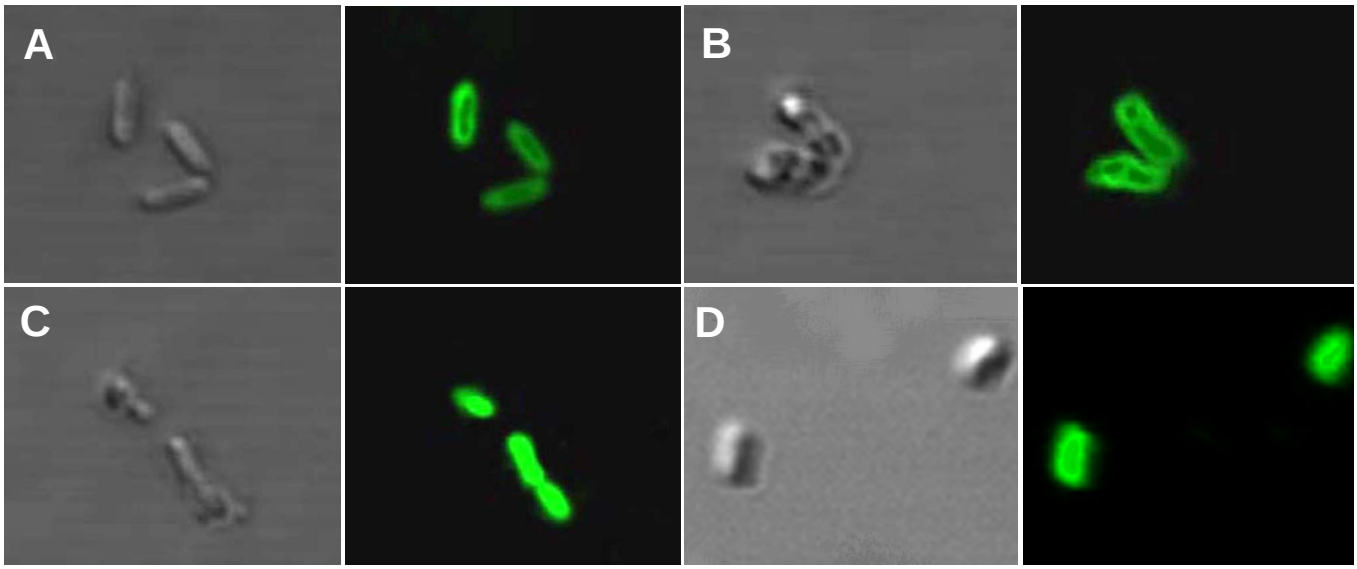


**Figure 7.** Confocal laser-scanning microscopy images of Gram-negative *E. coli* treated with FITC-labeled peptides. The cells were reacted with 5 μg/ml of FITC-labeled TP (A), FITC-labeled TPf (B), FITC-labeled TPk (C) or FITC-labeled TPK (D).

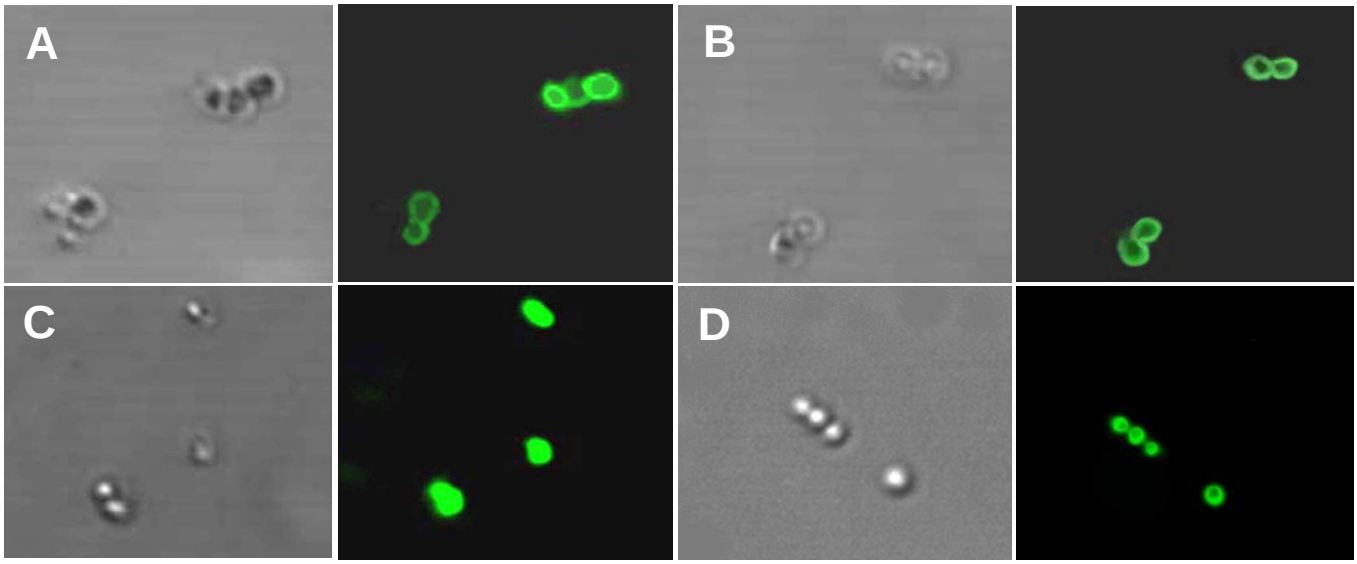


**Figure 8.** Confocal laser-scanning microscopy images of Gram-positive *S. aureus* treated with FITC-labeled peptides. The cells were reacted with 5 μg/ml of FITC-labeled TP (A), FITC-labeled TPf (B), FITC-labeled TPk (C) or FITC-labeled TPK (D).

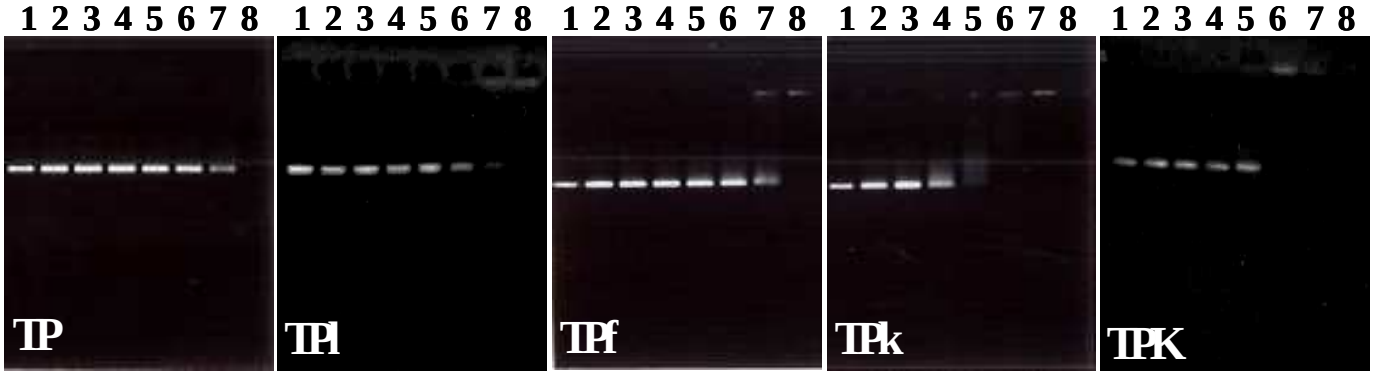


**Figure 9.** Interaction of the peptides with plasmid DNA. Binding was assayed by measuring the degree of inhibition of migration by plasmid DNA (100 ng; pBluscriptII $SK^+$): Lane 1, plasmid DNA alone; lane 2, 0.25 μM of peptide; lane 3, 0.5 μM of peptide; lane 4, 1.0 μM of peptide; lane 5, 2.0 μM of peptide; lane 6, 4.0 μM of peptide; lane 7, 8.0 μM of peptide; and lane 8, 16.0 μM of peptide. DNA and the peptides were co-incubated for 1 h at room temperature before electrophoresis on a 1.0 % agarose gel.

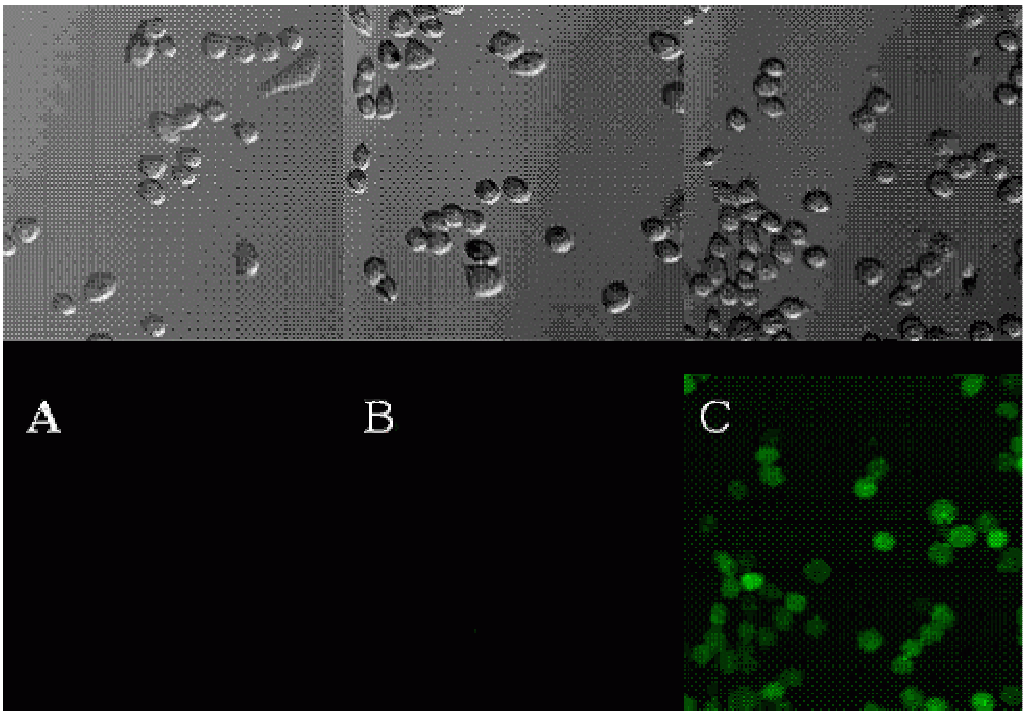


**Figure 10.** Peptide internalization and visualization assays in Hela cells by confocal laser-scanning microscope. HeLa cells were treated with FITC-labeled TP (A), FITC-labeled TPf (B) and FITC-labeled TPk (C) for 30 min at 37 °C. Final peptide concentration is 4 μM.

## Ⅳ. DISCUSSION

Proline is an amino acid that creates a bend in the peptide backbone because of its cyclic structure. Thus, the Pro residue is generally thought to be an α-helix breaker. Indeed, some of the naturally occurring α-helical antimicrobial peptides, such as cecropin A, pardaxin, and PMAP-23, contain one or two Pro residues (*5*, *28*). Due to the presence of a Pro residue near the central position, such antimicrobial peptides form a unique helix-bend-helix structure (*28-32*). Many studies have demonstrated that a Pro residue near the central position of these R-helical antimicrobial peptides plays an important role in their bacterial cell selectivity (*30-38*). In a recent study, we designed antimicrobial peptides containing peptoid residues with cell selectivity by incorporating one or two Nala residues into the hydrophobic helix of a non-cell-selective ideal amphiphatic LK-rich α-helical model peptide (*39*).

Due to the presence of the two Pro residues at positions 5 and 9, tritrpticin forms a unique turn-turn structure in the membrane-mimicking SDS micelles (*9*). The first turn consists of residues 4-7, followed immediately by a second well-defined $3_{10}$-helical turn consisting of residues 8-11. The hydrophobic residues are clustered together and are clearly separated from the basic Arg residues, resulting in an amphipathic structure. Peptoid residues, like proline, lack an amide nitrogen as a proton-donating group for hydrogen bonding to the peptide backbone. Thus, replacement of Pro residues with peptoid residues may also simultaneously induce a turn or a rigid bend in the secondary structure of the peptide (*40*).

In present study, to investigate the effect of Pro → peptoid residue substitution on the structure, cell selectivity, and mechanism of antibacterial action of a β-turn antimicrobial

peptide such as tritrpticin, tritrpticin-amide (TP) and its peptoid residue-substituted peptides (TPl, TPf, and TPk) were synthesized (Table 1). These studies were also carried out to provide information for the design new short antimicrobial peptides with selectivity for bacterial cells. As for TP, TPl and TPf displayed not only powerful antibacterial activity but also relatively strong hemolytic activity. In contrast, TPk had the most potent antimicrobial activity but lacked hemolytic activity even at 200 μM (Table 2, 3 and Figure 1). The cytotoxicity of the peptides was further examined by testing their ability to cause the lysis of human cervical carcinoma HeLa and mouse fibroblastic NIH-3T3 cells. All of the peptides were more cytotoxic to the transformed tumor HeLa cells than the normal NIH-3T3 cells. This may be due to the presence of a higher concentration of exposed anionic phospholipids on the outer membrane surface of transformed tumor cells than on normal cells (*41*, *42*). TPl and TPf not only had the highest hemolytic activity but also were the most cytotoxic against mammalian cells, whereas TPk did not exhibit significant cytotoxicitiy against either HeLa or NIH-3T3 cells at concentrations up to at least 100 μM (Table 4 and Figure 2).

To investigate whether the selectivity of TPk toward bacterial cells is related to differences in the interaction with the outer monolayer of membranes of bacterial and mammalian cells, tryptophan fluorescence quenching for each peptide in the presence of negatively charged model membranes (bacteria-mimicking membranes) and zwitterionic model membranes (mammalian-mimicking membranes) were studied. Unlike TP, TPl, and TPf, TPk effectively embedded the negatively charged membrane but not the zwitterionic membrane, suggesting that the selectivity of TPk toward bacterial cells is associated with a preferential interaction with negatively charged phospholipids (Table 5 and Figure 4).

Three general mechanisms, including barrel-stave, toroidal, and carpetlike models, were originally proposed to describe the process of permeabilization of the phospholipid membranes by membrane-active peptides (*28*, *43-47*). In the barrel-stave model, the peptide may create transmembrane channels or pores by forming bundles of amphipathic α-helices. In this case, the hydrophobic surfaces of the peptides may interact with the hydrophobic core of the membrane, while their hydrophilic surfaces face inward, producing an aqueous pore. The toroidal model differs from the barrel-stave model in that the lipid bends back on itself like the inside of a torus. Unlike the barrel-stave model where the peptide needs to be long enough to span the membrane, the toroidal model can be induced by smaller peptides because here the peptides probably play the role of stabilizing the lipid pore rather than lining the pore. In the carpet like model, the peptides lie at the interface parallel to the membrane, allowing their hydrophobic surfaces to interact with the hydrophobic component of the lipid, while their positively charged residues interact with the negatively charged head groups of the phospholipid.

In contrast to membrane-active peptides, other classes of antimicrobial peptides have been suggested to target nonmembrane intracellular components, such as DNA or RNA. PR-39, from porcine leucocytes (*48*), and buforin 2, from the stomach tissue of the Asian toad *Bufo bufo gargarizans* (*49*), are two peptides that penetrate cells without inducing severe membrane permeabilization. Once in the cytoplasm, they bind to and inhibit the activity of specific molecular targets essential to bacterial growth, thereby causing cell death (*49-54*).

The ability of TPk to cause leakage of a fluorescent dye entrapped within LUVs composed of negatively charged phospholipids was tested. Despite effectively binding and inserting into

negatively charged phospholipids, as demonstrated by tryptophan fluorescence blue shift and quenching experiments (Table 5 and Figure 4), TPk induced very little leakage of the dye from negatively charged phospholipid vesicles even at the highest concentration that was tested (10 μM) (Figure 5). To examine whether the cytoplasmic membrane of bacterial cells is the target of TPk, the abilities of the peptides to depolarize the cytoplasmic membrane of Gram-positive *S. aureus* and Gram-negative *E. coli* spheroplasts were examined by using the membrane potential-sensitive fluorescent dye $diSC_3$-5. The $diSC_3$-5 inserts into the cytoplasmic membrane under the influence of the membrane potential gradient and quenches its own fluorescence. After the addition of a peptide that forms a pore or channel or disrupts the membrane potential, the membrane potential is dissipated and the dye is released into the medium, leading to an increase in fluorescence. On the basis of the studies with this dye, TPk induced very little dissipation of the membrane potential even at levels 2-fold greater than the MIC against *S. aureus* and *E. coli* spheroplasts. In contrast, TP, TPl, TPf, and TPK caused a significant depolarization of the membrane under their MIC (Figure 6). These results suggested that the bactericidal action of TPk is not due to the formation of transmembrane channels or pores or the perturbation of the cell membrane.

The inability to cause leakage of calcein from bacterial membrane-mimicking liposomes and to depolarize *S. aureus* and *E. coli* spheroplast membranes prompted us to examine whether TPk is able to penetrate bacterial cell membranes. Therefore, we used confocal laser-scanning microscopy in conjunction with FITC-labeled peptides to determine whether the peptides penetrate bacterial cell membranes. FITC-labeled TPk penetrated the cell membrane and accumulated in the cytoplasm of both Gram-negative *E. coli* and Gram-positive *S. aureus*,

whereas neither FITC-labeled TP nor FITC-labeled TPf penetrated the cell membranes. Furthermore, in the gel retardation experiment, it was confirmed that TPk has a higher binding affinity for DNA. Taken together, these results indicated that TPk inhibits bacterial growth by intracellular targets like buforin 2 (*39*, *52-54*). Next, to investigate whether the ability of TPk to translocate across the bacterial cell membranes is due to only the increase in two positive charges, TPK with Lys at positions 5 and 9 of TP was synthesized and its biological functions were investigated. TPK induced rapid and effective leakage of dye from bacterial membrane-mimicking liposomes, and it effectively depolarized the cytoplasmic membrane of *S. aureus* and *E. coli* spheroplasts (Figures 5 and 6). Confocal laser-scanning microscopy revealed that TPK did not penetrate the cell membrane but remained outside or on the cell membrane (Figure 7 and 8). As mentioned earlier, despite the peptide's backbone change by Phe peptoid residue (Nphe) substitution, TPf did not translocate across the bacterial cell membranes. Taken together, these results suggested that the ability of TPk to penetrate into the bacterial cell membranes appears to be related to the dual effects that are related to the increase in the positive charge and the peptide's backbone change by peptoid residue substitution.

In conclusion, Pro → Nlys substitution (TPk) in TP significantly increased the antibacterial activity and decreased the cytotoxicity against mammalian cells, resulting in its cell selectivity. Unlike TP, TPl, TPf, and TPK, TPk caused very little dye leakage in negatively charged model membranes mimicking bacterial membranes. TPk also induced very little depolarization of the membrane potential in *S. aureus* and *E. coli* spheroplasts. Furthermore, TPk effectively penetrated the membranes of both Gram-negative *E. coli* and Gram-positive *S.*

*aureus* and bound strongly to DNA (Figure 9). These results suggest that the bactericidal effect of TPk is mediated by intracellular sites rather than by disruption of the exterior membrane. Further studies to identify an intracellular site to which TPk binds may reveal the mechanism of its bactericidal action. Interestingly, TPk also had the penetrating efficiency in mammalian cells (Figure 10). After further research about its internalization mechanism and its exact intracellular location, it maybe becomes a good cargo deliver in mammalian cells.

Collectively, our results demonstrate that a novel short antimicrobial peptide with high selectivity for bacterial cells and an intracellular mechanism of action can be generated by Pro → Nlys substitution in a Pro-containing β-turn antimicrobial peptide, such as tritrpticin. These findings help clarify the behavior of peptoid-containing antimicrobial peptides, and they provide a framework for the design of short synthetic antimicrobial peptides with optimized activity and selectivity profiles for possible therapeutic application. Particularly, TPk may be a suitable lead compound for the development of cell-selective antimicrobial peptides.

## Ⅴ. REFERENCES


1. Boman, H. G. (1995) Peptide antibiotics and their role in innate immunity, *Annu. Rev. Immunol. 13*, 61-92.
2. Zasloff, M. (2002) Antimicrobial peptides of multicellular organisms, *Nature 415*, 389-395.
3. Hancock, R. E., and Scott, M. G. (2000) The role of antimicrobial peptides in animal defenses, *Proc. Natl. Acad. Sci. U.S.A. 97*, 8856-8861.
4. Hancock, R. E., and Diamond, G. (2000) The role of cationic antimicrobial peptides in innate host defences, *Trends Microbiol. 8*, 402-410.
5. Andreu, D. and Rivas, L. (1998) Animal antimicrobial peptides: an overview, *Biopolymers 47*, 415-433.
6. Lawyer, C., Pai, S., Watabe, M., Borgia, P., Mashimo, T., Eagleton, L.,and Watabe, K. (1996) Antimicrobial activity of a 13 amino acid tryptophan-rich peptide derived from a putative porcine precursor protein of a novel family of antibacterial peptides, *FEBS Lett. 390*, 95-98.
7. Yang, S. T., Shin, S. Y., Kim, Y. C., Kim, Y., Hahm, K. -S., and Kim, J. I. (2002) Conformation-dependent antibiotic activity of tritrpticin, a cathelicidin-derived antimicrobial peptide, *Biochem. Biophys. Res. Commun. 296*, 1044-1050.
8. Yang, S. T., Shin, S. Y., Lee, C. W., Kim, Y. C., Hahm, K. -S., and Kim, J. I. (2003) Selective cytotoxicity following Arg-to-Lys substitution in tritrpticin adopting a unique amphipathic turn structure, *FEBS Lett. 540*, 229-233.

9. Schibli, D. J., Hwang, P. M.,and Vogel, H. J. (1999) Structure of the antimicrobial peptide tritrpticin bound to micelles: a distinct membrane-bound peptide fold, *Biochemistry 38*, 16749-16755.

10. Wu, C. W., Sanborn, T. J., Zuckermann, R. N., and Barron, A. E. (2001) Peptoid oligomer with α-chiral, aromatic side chains: Effects of chain length on secondary structure, *J. Am. Chem. Soc. 123*, 2958-2963.

11. Ng, S., Goodson, B., Ehrhardt, A., Moos, W. H., Siani, M., and Winter, J. (1999) Combinatorial discovery process yields antimicrobial peptoids, *Bioorg. Med. Chem. 7*, 1781-1785.

12. Wender, P. A., Mitchell, D. J., Pattabiraman, K., Pelkey, E. T., Steinman, L., and Rothbard, J. B. (2000) The design, synthesis, and evaluation of molecules that enable or enhance cellular uptake: Peptoid molecular transporters, *Proc. Natl. Acad. Sci. U.S.A. 97*, 13003-13008.

13. Goodman, M., Bhumralkar, Jefferson, E. A., Kwak, J., and Locardi, E. (1998) Collagen mimetics, *Biopolymers 47*, 127-142.

14. Tang, Y. C., and Deber, C. M. (2002) Hydrophobicity and helicity of membrane-interactive peptides containing peptoid residues, *Biopolymers 65*, 254-262.

15. Tang, Y. C., and Deber, C. M. (2004) Aqueous solubility and membrane interactions of hydrophobic peptides with peptoid tags, *Biopolymers 76*, 110-118.

16. Scudiero, D. A., Shoemaker, R. H., Paull, K. D., Monks, A., Tierney, S., Nofziger, T. H., Currens, M. J., Seniff, D., and Boyd, M. R. (1988) Evaluation of a soluble

tetrazolium/formazan assay for cell growth and drug sensitivity in culture using human and other tumor cell lines, *Cancer Res. 48*, 4827-4833.

17. Mao, D.,and Wallace, B. A. (1984) Differential light scattering and absorption flattening optical effects are minimal in the circular dichroism spectra of small unilamellar vesicles, *Biochemistry 23*, 2667-2673.
18. Shai, Y., Bach, D.,and Yanovsky, A. (1990) Channel formation properties of synthetic pardaxin and analogues, *J. Biol. Chem. 265*, 20202-20209.
19. De Kroon, A. I., Soekarjo, M. W., De Gier, J., and De Kruijff, B. (1990) The role of charge and hydrophobicity in peptide-lipid interaction: a comparative study based on tryptophan fluorescence measurements combined with the use of aqueous and hydrophobic quenchers, *Biochemistry 29*, 8229-8240.
20. Zhao, H., and Kinnunen, P. K. (2002) Binding of the antimicrobial peptide temporin L to liposomes assessed by Trp fluorescence, *J. Biol. Chem. 277*, 25170-25177.
21. Papo, N., Oren, Z., Pag, U., Sahl, H.-G., and Shai, Y. (2002) The consequence of sequence alternation of amphipathic α-helical antimicrobial peptide and its diasteromers, *J. Biol. Chem. 277*, 33913-33921.
22. Sal-Man, N., Oren, Z., and Shai, Y. (2002) Preassembly of membrane-active peptides is an important factor in their selectivity toward target cells, *Biochemistry 41*, 11921-11930.
23. Shin, S. Y., Kang, S. W., Lee, D. G., Eom, S. H., Song, W. K., and Kim, J. I. (2000) CRAMP analogues having potent antibiotic activity against bacterial, fungal, and tumor cells without hemolytic activity, *Biochem. Biophys. Res. Commun. 275*, 904-909.

24. Shin, S. Y., Kang, J. H., Jang, S. Y., Kim. Y., Kim, K. L., and Hahm, K. -S. (2000) Effects of the hinge region of cecropin A(1-8)-magainin 2(1-12), a synthetic antimicrobial peptide, on liposomes, bacterial and tumor cells, *Biochim. Biophys. Acta 1463*, 209-218.

25. Shin, S. Y., Lee, S. H., Yang, S. -T., Park, E. J., Lee, D. G., Lee, M. K., Eom, S. H., Song, W. K., Kim, Y., Hahm, K. -S., and Kim, J. I. (2001) Antibacterial, antitumor and hemolytic activities of alpha-helical antibiotic peptide, P18 and its analogs, *J. Pept. Res. 58*, 504-514.

26. Woody, R. W. (1994) Contributions of tryptophan side chains to the far-ultraviolet circular dichroism of proteins, *Eur. Biophys. J. 23*, 253-262.

27. Nagpal, S., Gupta, V., Kaur, K. J.,and Salunke, D. M. (1999) Structure-function analysis of tritrypticin, an antibacterial peptide of innate immune origin, *J. Biol. Chem. 24*, 23296-23304.

28. Tossi, A., Sandri, L., and Giangaspero, A. (2000) Amphipathic, α-helical antimicrobial peptides, *Biopolymers 55*, 4-30.

29. Holak, T. A., Engstrom, A., Kraulis, P. J., Lindeberg, G., Bennich, H., Jones, T. A., Gronenborn, A. M., and Clore, G. M. (1988) The solution conformation of the antibacterial peptide cecropin A: a nuclear magnetic resonance and dynamical simulated annealing study, *Biochemistry 27*, 7620-7629.

30. Park, K., Oh, D., Shin, S. Y., Hahm, K. -S. and Kim, Y. (2002) Structural studies of porcine myeloid antibacterial peptide PMAP-23 and its analogues in DPC micelles by NMR spectroscopy, *Biochem. Biophys. Res. Commun. 290*, 204-212.

31. Thennarasu, S.,and Nagaraj, R. (1996) Specific antimicrobial and hemolytic activities of 18-residue peptides derived from the amino terminal region of the toxin pardaxin, *Protein Eng. 9*, 1219-1224.

32. Suh, J. Y., Lee, Y. T., Park, C. B., Lee, K. H., Kim, S. C., and Choi, B. S. (1999) Structural and functional implications of a proline residue in the antimicrobial peptide gaegurin, *Eur. J. Biochem. 266*, 665-674.

33. Shin, S. Y., Park, E. J., Yang, S. -T., Jung, H. J., Eom, S. H., Song, W. K., Kim, Y., and Hahm, K. -S., and Kim, J. I. (2001) Structural and functional implications of a proline residue in the antimicrobial peptide gaegurin, *Biochem. Biophys. Res. Commun. 285*, 1046-1051.

34. Oh, D., Shin, S. Y., Lee, S., Kang, J. H., Kim, S. D., Ryu, P. D., Hahm, K. -S., and Kim, Y. (2000) Role of the hinge region and the tryptophan residue in the synthetic antimicrobial peptides, cecropin A(1-8)-magainin 2(1-12) and its analogues, on their antibiotic activities and structures, *Biochemistry 39*, 11855-11864.

35. Song, Y. M., Yang, S. -T., Lim, S. S., Kim, Y., Hahm, K. -S., Kim, J. I., and Shin, S. Y. (2004) Effects of L- or D-Pro incorporation into hydrophobic or hydrophilic helix face of amphipathic α-helical model peptide on structure and cell selectivity, *Biochem. Biophys. Res. Commun. 314*, 615-621.

36. Lee, K., Shin, S. Y., Kim, K., Lim, S. S., Hahm, K. -S., and Kim, Y. (2004) Antibiotic activity and structural analysis of the scorpion-derived antimicrobial peptide IsCT and its analogs, *Biochem. Biophys. Res. Commun. 323*, 712-719.

37. Pukala, T. L., Brinkworth, C. S., Carver, J. A.,and Bowie, J. H. (2004) Investigating the importance of the flexible hinge in caerin 1.1: solution structures and activity of two synthetically modified caerin peptides, *Biochemistry 43*, 937-944.

38. Lim, S. S., Kim, Y., Park, Y., Kim, J. I., Park, I. -S., Hahm, K. -S., and Shin, S. Y. (2005) The role of the central L- or D-Pro residue on structure and mode of action of a cell-selective alpha-helical IsCT-derived antimicrobial peptide, *Biochem. Biophys. Res. Commun. 334*, 1329-1335.

39. Song, Y. M., Park, Y., Lim, S. S., Yang, S. -T. Woo, E. -R. Park, I. -S., Lee, J. S., Kim, J. I., Hahm, K. -S., Kim, Y., and Shin, S. Y. (2005) Cell selectivity and mechanism of action of antimicrobial model peptides containing peptoid residues, *Biochemistry 44*, 12094-12106.

40. Rainaldi, M., Moretto, V., Crisma, M., Peggion, E., Mammi, S., Toniolo, C., and Cavicchioni, G. (2002) Peptoid residues and β-turn formation, *J. Pept. Sci. 8*, 241-252.

41. Connor, J., Bucana, C., Fidler, I. J., and Schroit, A. J. (1989) Differentiation-dependent expression of phosphatidylserine in mammalian plasma membranes: Quantitative assessment of outerleaflet lipid by prothrombinase complex formation, *Proc. Natl. Acad. Sci. U.S.A. 86*, 3184-3188.

42. Utsugi, T., Schroit, A. J., Connor, J., Bucana, C. D., and Fidler, I. J. (1991) Elevated expression of phosphatidylserine in the outer membrane leaflet of human tumor cells and recognition by activated human blood monocytes, *Cancer Res. 51*, 3062-3066.

43. Oren, Z., and Shai, Y. (1998) Mode of action of linear amphipathic alpha-helical antimicrobial peptides, *Biopolymers 47*, 451-463.

44. Shai, Y., and Oren, Z. (2001) From "carpet" mechanism to de-novo designed diastereomeric cell-selective antimicrobial peptides, *Peptides 22*, 1629-1641.

45. Shai, Y. (2002) Mode of action of membrane active antimicrobial peptides, *Biopolymers 66*, 236-248.

46. Papo, N., and Shai, Y. (2003) Can we predict biological activity of antimicrobial peptides from their interactions with model phospholipid membranes? *Peptides 24*, 1693-1703.

47. Agerberth, B., Lee, J. Y., Bergman, T., Carlquist, M., Boman, H. G., Mutt, V., and Jornvall, H. (1991) Amino acid sequence of PR-39. Isolation from pig intestine of a new member of the family of proline-arginine-rich antibacterial peptides, *Eur. J. Biochem. 202*, 849-854.

48. Agerberth, B., Lee, J. Y., Bergman, T., Carlquist, M., Boman, H. G., Mutt, V., and Jornvall, H. (1991)Amino acid sequence of PR-39. Isolation from pig intestine of a new member of the family of proline-arginine-rich antibacterial peptides, *Eur. J. Biochem. 202*, 849-854.

49. Park, C. B., Kim, M. S., and Kim, S. C. (1996) A novel antimicrobial peptide from Bufo bufo gargarizans, *Biochem. Biophys. Res. Commun. 218*, 408-413.

50. Boman, H. G., Agerberth, B., and Boman, A. (1993) Mechanisms of action on *Escherichia coli* of cecropin P1 and PR-39, two antibacterial peptides from pig intestine, *Infect. Immun. 61*, 2978-2984.

51. Gennaro, R., Zanetti, M., Benincasa, M., Podda, E., and Miani, M. (2002) Pro-rich antimicrobial peptides from animals: structure, biological functions and mechanism of action, *Curr. Pharm. Des. 8*, 763-778.

52. Park, C. B., Kim, H. S., and Kim, S, C. (1998) Mechanism of action of the antimicrobial peptide buforin II: buforin II kills microorganisms by penetrating the cell membrane and inhibiting cellular functions, *Biochem. Biophys. Res. Commun. 244*, 253-257.

53. Park, C. B., Yi, K. S., Matsuzaki, K., Kim, M. S.,and Kim, S. C. (2000) Structure-activity analysis of buforin II, a histone H2A-derived antimicrobial peptide: the proline hinge is responsible for the cell-penetrating ability of buforin II, *Proc. Natl. Acad. Sci. U.S.A. 97*, 8245-8250.

54. Kobayashi, S., Takeshima, K., Park, C. B., and Kim, S. C., and Matsuzaki, K. (2000) Interactions of the novel antimicrobial peptide buforin 2 with lipid bilayers: proline as a translocation promoting factor, *Biochemistry 39*, 8648-8654.

## Ⅵ. ACKNOWLEDGMENT

I would very much like to express my gratitude to my supervisor, Prof. Song Yub Shin for his support and experimental guidance thorough the duration of this study. I want to thank Prof. Kyung-Soo Hahm and Prof. Il-Seon Park for their contribution as examiners of this thesis. I would also like to thank Miss Shin Saeng Lim and Miss Yun Mi Song for providing useful experimental instructions, as well as Dr. Alan K Chang for reviewing this thesis. Finally, I would like to thank my parents for their strong and continuous moral support for my study and my life here in Korea.

## Ⅶ. ABBREVIATIONS

CD, Circular cichroism;

CFU, colony-forming unite;

CPPs, cell-penetrating peptides;

di$SC_3$-5, 3,3'-dipropylthiadicarbocyanine iodide;

DMEM, Dulbecco's modified Eagle's medium;

EYPC, egg yolk L-α-phosphatidylcholine;

EYPG, egg yolk L-phosphatidyl-DL-glycerol;

FBS, fetal bovine serum;

FITC, fluorescein isothiocyanate;

Fmoc, fluoren-9-yl-methoxycarbonyl;

h-RBC, human red blood cells;

LUVs, large unilamellar vesicles;

MALDI-TOF MS, matrix-assisted laser-desorption ionization-time-of-flight mass spectrometry;

MIC, minimal inhibitory concentration;

MTT, 3-(4,5-dimethylthiazol-2-yl)-2,5-diphenyl-2H-tetrazolium bromide;

RP-HPLC, reverse phase high-performance liquid chromatography;

PBS, phosphate buffered saline;

SDS, sodium dodecyl sulfate;

SUVs, small unilamellar vesicles.

## (국문 초록)

# 항균펩타이드 tritrpticin-amide 의 구조, 세포특이성 및 항균작용기작에 있어서 proline 의 peptoid 잔기로의 치환이 미치는 영향

주 만 용

조선대학교 대학원

생물신소재 학과

(지도교수: 신 송 엽)

본 연구에서는 proline 을 포함하는 β-turn 항균 펩타이드에 있어서 proline 의 peptoid residue 로의 치환이 세균특이성 및 항균작용기작에 미치는 영향을 조사하기 위하여, 항균 펩타이드 tritrpticin-amide (TP; VRRFPWWWPFLRR-$NH_2$) 및 TP 의 5, 9 번째에 있는 2 개의 proline 잔기를 Ala-peptiod residue (Nala), Leu-peptiod residue (Nleu), Phe-peptiod residue (Nphe), Lys-peptiod residue (Nlys)로 각각 치환시킨 펩타이드를 합성하였다.

TP 의 proline 을 Nala, Nleu 또는 Nphe 로 치환시킨 펩타이드(TPa, TPl 및 TPf)는 거의 박테리아의 항균활성이 유지되었으나 포유동물세포(mammalian cells)에 있어서의 강한 세포독성(cytotoxicity)을 나타내었다. 반면에 proline 의 Nlys 로의 치환 (TPk)은 항균활성을 증가시켰으며, 포유동물세포에 대한 세포독성을 현저히 감소시켰다.

트립토판 형광실험 (Tryptophan fluorescence experiment)을 통하여 항균 펩타이드 TPk 의 박테리아 세포특이성은 negatively charged phospholipid 에 대한 우선적 상호작용과 관련성이 있다는 사실을 알았다. 흥미롭게도, TPk 는 *Staphylococcus aureus* 에 대한 membrane deploarization 활성 및 negatively charged vesicle 내에 포획된 fluorescent dye 의 leakage 활성에 있어서 매우 덜 효과적이였다. 더구나, confocal laser-scanning microscopy 를 통하여 항균 펩타이드 TPk 는 *Escherichia coli* 및 *Staphylococcus aureus* 의 세포막을 통과하여 세포질내에 축적되지만, TP 및 TPf 는 세포막을 통과하지 않고 세포막 표면이나 외부에 결합된다는 사실을 알았다.

Gel retardation assay 를 통하여 항균 펩타이드 TPk 는 TP 및 TPf 보다 매우 강한 DNA 결합능력을 보였다. 이들 결과로부터 TPk 의 살균작용기작은 세균세포막을 통과한 후, 세포내 표적 (intracellular target)의 저해에 의한 것임을 시사하였다. 또한 TP 에 있어서 proline 을 lysine 으로 치환시킨 펩타이드 TPK 는 *Staphylococcus aureus* 의 cytoplasmic membrane 을 효과적으로 depolarization 시킨다는 사실을 알았다. TPK 는 박테리아 세포막을 모방하는 리포좀 (bacterial membrane-mimicking liposome)으로부터 빠르고, 효과적인 dye leakage 를 유도하였다. 이 사실은 항균 펩타이드 TPk 의 박테리아 세포막에 효과적인 통과(penetration)는 Lys peptoid

residue 의 치환에 의한 positive charge 의 증가 및 펩타이드의 backbone change 에 관련된 이중효과 때문이라는 사실을 시사하였다.

이상의 연구 결과로부터 tritrpticin 과 같이 proline 을 포함하는 β-turn 구조 항균 펩타이드에 있어서 proline 잔기의 Lys peptoid residue (Nlys)로의 치환은 세포내 표적 작용기작 (intracellular target mechanism)을 나타내는 새로운 박테리아세포 특이성 항균 펩타이드의 설계를 위한 유용한 수단임을 알았다.

(별 지)

**저작물 이용 허락서**

| 학 과 | 생물신소재 | 학 번 | 20047658 | 과 정 | 석사 |
|---|---|---|---|---|---|
| 성 명 | 한글: 주 만 용 한문: 朱 萬 龍 영문: Zhu Wang Long | | | | |
| 주 소 | 광주광역시 동구 서석동 375 조선대학교 Green House 남자기숙사 412 호 | | | | |
| 연락처 | E-MAIL : wlz1981@hotmail.com | | | | |
| 논문제목 | 한글: 항균펩타이드 tritrpticin-amide 의 구조, 세포특이성 및 항균작용기작에 있어서 proline 의 peptoid 잔기로의 치환이 미치는 영향<br>영문: Effect of Proline to Peptoid Residue Substitution on the Structure, Cell Selectivity and Mechanism of Antibacterial Action of Antimicrobial Peptide Tritrpticin-amide | | | | |

본인이 저작한 위의 저작물에 대하여 다음과 같은 조건아래 -조선대학교가 저작물을 이용할 수 있도록 허락하고 동의합니다.

- 다 음 -

1. 저작물의 DB 구축 및 인터넷을 포함한 정보통신망에의 공개를 위한 저작물의 복제, 기억장치에의 저장, 전송 등을 허락함

2. 위의 목적을 위하여 필요한 범위 내에서의 편집・형식상의 변경을 허락함. 다만, 저작물의 내용변경은 금지함.

3. 배포・전송된 저작물의 영리적 목적을 위한 복제, 저장, 전송 등은 금지함.

4. 저작물에 대한 이용기간은 5 년으로 하고, 기간종료 3 개월 이내에 별도의 의사표시가 없을 경우에는 저작물의 이용기간을 계속 연장함.

5. 해당 저작물의 저작권을 타인에게 양도하거나 또는 출판을 허락을 하였을 경우에는 1 개월 이내에 대학에 이를 통보함.

6. 조선대학교는 저작물의 이용허락 이후 해당 저작물로 인하여 발생하는 타인에 의한 권리 침해에 대하여 일체의 법적 책임을 지지 않음

7. 소속대학의 협정기관에 저작물의 제공 및 인터넷 등 정보통신망을 이용한 저작물의 전송・출력을 허락함.

년 월 일